

Robust Control of an Input-redundant Aircraft against Atmospheric Disturbances and Actuator Faults

Maksim Trifonov

Department of System Analysis and Control, Moscow Aviation Institute (National Research University), Moscow, Russia

Email: trifonov.m@yahoo.com

Karl Frederik Prochazka and Saleh Krüger

Institute of Flight Systems and Automatic Control, Technische Universität Darmstadt, Darmstadt, Germany

Email: {prochazka, krueger}@fsr.tu-darmstadt.de

Abstract—There are several applications for modern robust control theory in which closed-loop performance in the face of model uncertainties and measurement noise is of uttermost importance. Especially for safety-critical areas like aerospace systems uncertainties due to unmodeled dynamics or neglected flexible modes as well as atmospheric disturbances have to be carefully considered during the controller design procedure. Another important aspect in flight control system (FCS) design is fault-tolerance. As many modern aircrafts are inherently over-actuated, the control objective could still be achieved when one or even more actuators fail. It is thus of practical interest to extend the robust controller's performance analysis to also incorporate such scenarios. This paper presents the design of a robust longitudinal controller for the input-redundant ADMIRE (Aero-Data Model in Research Environment) aircraft benchmark model. After the analysis of the closed-loop system's performance in the simultaneous presence of aerodynamic uncertainties, sensor noise and turbulence acting on the aircraft, the additional occurrence of actuator faults has been simulated to determine the FCS's robust stability margins.

Index Terms— H_∞ control, robust analysis, aerodynamic uncertainty, atmospheric turbulence

I. INTRODUCTION

One of the key problems for the design and simulation of aerial vehicle's (AV) motion control algorithms is the consideration of uncertainties – both internal uncertainties in the AV motion model itself (due to aerodynamic variation, measurement errors etc.) [1-2] and external uncertainties from the environment like atmospheric turbulence [3-4]. There are structural and parametric uncertainties [5] and each type of uncertainties can cause a critical discrepancy between AV flight data and the data received from the simulated motion. Such discrepancy can cause the non-fulfillment of the flight task or even an accident. The origin of

uncertainties can be diverse: for example, they might stem from wind gusts or when it is necessary to change parameters of the AV abruptly (e.g. flight altitude, angle of attack etc.). In such cases bending moments of the AV's structure might appear [6] what leads to the dispersion of its aerodynamic properties [1]. Further, engine failures can cause vibrations appearing in the AV's structure which will affect the measurement accuracy of navigation sensors [7]. In some cases the presence of uncertainties can cause a number of successive negative effects, particularly, an additional disturbing moment because of asymmetric impact of uncertainties [5].

As the requirement for system reliability is ever increasing while application areas for modern aircraft systems are growing constantly, more sophisticated control methods than classical PID control or LQR become necessary. For this purpose the utilization of robust control theory [8] presents a good choice, where the synthesis of AV motion control algorithms is based on the plant model's properties in the frequency domain. When applying robust control methods to a particular plant model with a given set of uncertainties one of the main tasks is to evaluate the performance of the suggested control algorithms as part of a closed-loop perturbed AV model. To the effective methods of robust controller design belongs the method of H_∞ control, particularly the method suggested by McFarlane and Glover [9-10]. A classic version of this method was later called H_∞ normalized coprime factorization [11]. One of its modifications developed by Le and Safonov [12-13] is called H_∞ optimal loop-shaping control. The advantage of both approaches is that the uncertainty model doesn't represent any real physical uncertainty which is actually unknown. Such approaches only require a desired form of the open-loop transfer function in the frequency domain. The disadvantage of such synthesis methods is the possible high dimensionality of the designed controllers

[14]. In this case appropriate methods to reduce the controller's order are available.

When developing motion control algorithms of AV, special attention should be paid to the class of systems that are designed with a marginal static stability or even unstable behavior to achieve greater maneuverability [15]. For such aircrafts like the HIMAT [14] and F-16 aircraft [16], robust control methods have already been applied. The occurrence of uncertainties and impact of external disturbances like turbulences on an AV might also have a chain effect that could lead to a simultaneous impact of several uncertainties on the examined system [17]. Such situations can lead to a broad variation of the AV's aerodynamic properties and thus to a high risk of losing control over the system.

To maintain at best nominal performance of the closed-loop system in the presence of a failure, the FCS also has to be fault-tolerant [18]. One of the main requirements for fault-tolerant control (FTC) is the redundancy of actuators (or sensors), which can either be based on physical or analytical redundancy [18]. FTC systems can typically be divided into active and passive approaches, where the former reacts to occurrence of a fault by actively changing the underlying control system and thus being able to (at best) maintain nominal performance. This requires the implementation of an appropriate fault detection and reconfiguration scheme, though. The implementation of a robust fault detection approach with optimization-based control reconfiguration has been presented in [19]. For passive FTC no additional components have to be designed. Here a fixed controller structure is used, which typically incorporates faults and uncertainties in a robust design approach.

The purpose of this paper is to analyze the fault-tolerance capabilities of a passive AV motion controller based on a robust H_∞ analysis and synthesis procedure. For the simulations a benchmark aircraft model with unstable longitudinal modes and input-redundancy has been used [20]. To demonstrate the robustness properties of the presented method aerodynamic uncertainties and sensor noise as well as turbulences have been simulated. Finally, actuator faults have been added to the simulations.

This paper is organized as follows. In section II the implemented robust H_∞ control methods are presented. Section III introduces the aircraft benchmark model on which the robust control scheme has been simulated. In section IV the implemented simulation setup is shown. Furthermore the design of two robust controller as well as a PID benchmark controller is described. The different simulations and results are presented in section V. Finally, section VI concludes the paper and gives an outlook on possible future extensions of the presented work.

II. ADMIRE AIRCRAFT MODEL

The subject of research of this paper is the ADMIRE aircraft model which represents a generic nonlinear six degree of freedom high-speed delta canard aircraft as

given in Fig. 1. The ADMIRE aircraft model has been designed by FOI, Sweden [20-21].

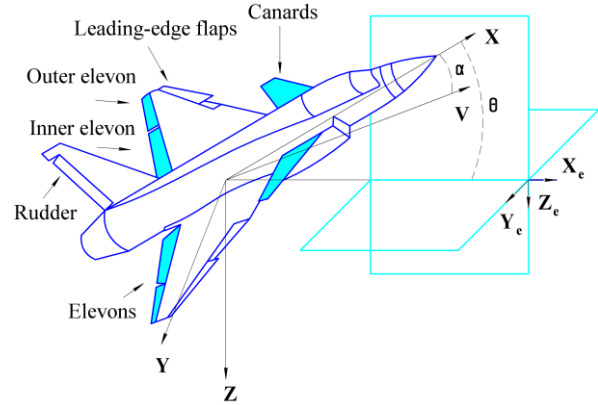


Figure 1. Configuration of the ADMIRE aircraft (colored areas are longitudinal control inputs).

This paper examines a simplified model of the ADMIRE aircraft with the following assumptions:

- the aircraft is trimmed at a steady-state horizontal flight;
- control in the longitudinal axis is realized by means of elevons and canards;
- a synchronous deflection of each actuator pair (outer and inner elevons and canards) is assumed.

A nonlinear model of ADMIRE aircraft longitudinal motion can be presented as a system of 5 differential equations:

$$\begin{aligned}\dot{V} &= (-F_D + F_T \cos \alpha - F_g \sin(\theta - \alpha)) / m, \\ \dot{\alpha} &= q + (-F_L - F_T \sin \alpha + F_g \cos(\theta - \alpha)) / mV, \\ \dot{q} &= (M_{Ay} + M_{Ty}) / I_y, \\ \dot{\theta} &= q, \\ \dot{h} &= -z,\end{aligned}\quad (1)$$

where $F_L = C_L \alpha S \rho V^2 / 2$, $F_D = C_D S \rho V^2 / 2$ are aerodynamic lift and drag forces; $M_{Ay} = C_M \bar{c} S \rho V^2 / 2$, $M_{Ty} = F_T z_T$ are aerodynamic and thrusting moments; F_T is thrust force; z_T is moment arm of F_T ; F_g is force of gravity; C_L, C_D, C_M are the corresponding aerodynamic coefficients; V is the airspeed (m/s), \bar{c} is the aerodynamic chord (m), q is pitch rate (deg/s), S is the wing area (m²), ρ is the air mass density (kg/m³), α is angle of attack (deg); θ is pitch angle (deg), m is mass of the aircraft (kg), z is height (m) and I_y is pitch inertia (kg·m²).

For a preliminary analysis, the equation system (1) can be presented as a linear system of the following form:

$$\begin{aligned}\dot{\mathbf{x}}(t) &= \mathbf{A}\mathbf{x}(t) + \mathbf{B}_w \mathbf{w}(t) + \mathbf{B}_u \mathbf{u}(t), \\ \mathbf{z}(t) &= \mathbf{C}_z \mathbf{x}(t) + \mathbf{D}_{w1} \mathbf{w}(t) + \mathbf{D}_{u1} \mathbf{u}(t), \\ \mathbf{y}(t) &= \mathbf{C}_y \mathbf{x}(t) + \mathbf{D}_{w2} \mathbf{w}(t) + \mathbf{D}_{u2} \mathbf{u}(t),\end{aligned}\quad (2)$$

where $\mathbf{x} = [\Delta V \ \Delta \alpha \ q \ \Delta \theta \ \Delta h]^T_{5 \times 1}$ is the state vector, $\mathbf{u} = [\delta_c \ \delta_{ie} \ \delta_{oe}]^T_{3 \times 1}$ is the control input, δ_c is the canard angle (deg), δ_{ie} is the inner elevon angle (deg), δ_{oe} is the

outer elevon angle (*deg*), $\mathbf{r} = [\alpha_{ref} \ \theta_{ref}]^T$ is the reference vector, $\mathbf{n} = [n_\alpha \ n_\theta]^T$ is the measurement noise vector, $\mathbf{w}_{turb} = [w_x \ w_z]^T$ is the turbulence vector, $\mathbf{w} = [\mathbf{w}_{turb}^T \ \mathbf{n}^T]^T$ is the disturbance vector, $\mathbf{z} = [\Delta\alpha \ \Delta\theta]^T$ is the vector of controlled variables, $\mathbf{y} = [\tilde{\alpha} \ \tilde{\theta}]^T = [(\Delta\alpha + n_\alpha) \ (\Delta\theta + n_\theta)]^T$ is the measured output vector.

III. ROBUST H_∞ CONTROL METHOD

This paper examines a MIMO system whose structure in robust control applications usually has a form as presented in Fig. 2. The input and output parameters are presented in detail in section II. The \mathbf{K}_∞ controller is a robust H_∞ controller, Δ is the uncertainty of the aerodynamic coefficients C_L, C_D, C_M and \mathbf{P} is the linear model of the ADMIRE aircraft in matrix form:

$$\mathbf{P} = \begin{bmatrix} \mathbf{P}_{11} & \mathbf{P}_{12} \\ \mathbf{P}_{21} & \mathbf{P}_{22} \end{bmatrix} = \begin{bmatrix} \mathbf{A} & \mathbf{B}_w & \mathbf{B}_u \\ \mathbf{C}_z & \mathbf{D}_{w1} & \mathbf{D}_{u1} \\ \mathbf{C}_y & \mathbf{D}_{w2} & \mathbf{D}_{u2} \end{bmatrix}$$

The main problem of H_∞ optimization approach is that the closed-loop system should comply with both requirements for robustness and for efficiency. To achieve this the H_∞ norm be limited:

$$\|\mathbf{N}(s)\|_\infty = \left\| \begin{bmatrix} \mathbf{S}(s)\mathbf{W}_1(s) \\ \mathbf{T}(s)\mathbf{W}_2(s) \\ \mathbf{R}(s)\mathbf{W}_3(s) \end{bmatrix} \right\|_\infty \leq \gamma, \quad (3)$$

where $\mathbf{S}(s)$ is the sensitivity matrix defining the robust quality. $\mathbf{T}(s)$ is the complementary sensitivity matrix that secures the robust stability of the system. $\mathbf{R}(s)$ is the control sensitivity matrix and γ is a loop-shaping accuracy. $\mathbf{W}_1(s), \mathbf{W}_2(s), \mathbf{W}_3(s)$ are weighting transfer functions that define desired frequency properties of tracking error signals, monitored outputs and control, respectively. In the design process the desired singular values of \mathbf{L}, \mathbf{S} and \mathbf{T} are specified, with $\mathbf{L}(s)$ being the loop transfer function matrix $\mathbf{L}(s) = \mathbf{P}(s)\mathbf{K}(s)$.

The paper examines two methods of robust controller synthesis: H_∞ normalized coprime factorization ($H_{\infty,ncf}$) and H_∞ loop-shaping synthesis ($H_{\infty,loop}$). The uncertainties in the $H_{\infty,ncf}$ approach are simulated as coprime uncertainties. This approach only requires a desired form of the open-loop system in the frequency domain. Two weighting functions, $\mathbf{W}_{p1}(s)$ (pre-compensator) and $\mathbf{W}_{p2}(s)$ (post-compensator), are given to form a nominal \mathbf{P} in order to reach a desired form of the open-loop system. This robust synthesis method comprises 5 successive steps defined in [14].

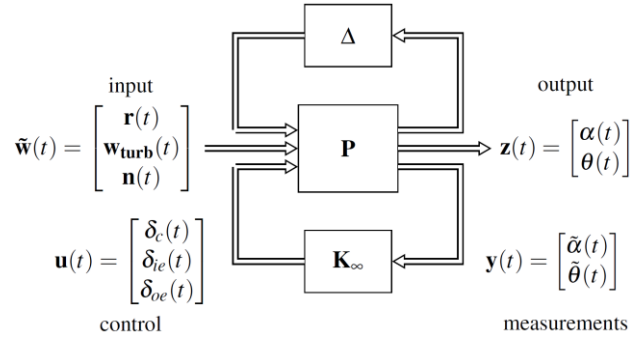


Figure 2. The classical structure of a closed-loop MIMO system the robust control theory.

The $H_{\infty,loop}$ method, introduced by Safonov and Le, is used to compute a Glover-McFarlane pre-filter $\mathbf{W}_{p1}(s)$. The pre-filter is then used to assume any specified loop-shape $|\mathbf{G}_d(j\omega)|$ [13, 22]. The derived Safonov-Le pre-filter allows to design an optimal loop-shaping controller for a MIMO plant \mathbf{P} without the need of manually computing the weight matrix $\mathbf{W}_{p1}(s)$. Using the *loopsyn* function in MATLAB a desired loop-shape \mathbf{G}_d can be specified and implemented easily by providing the characterizing cutoff frequency of \mathbf{G}_d .

IV. CONTROLLER DESIGN

For the following examinations the ADMIRE aircraft model is linearized at a height of $h = 6000$ (m) and an airspeed of Mach $M = 1$. The linearized model is open-loop unstable. The components of the system (2) are of the following form:

- System matrix

$$\mathbf{A} = \begin{bmatrix} -0.0937 & 1.0669 & -0.0237 & -9.8100 & 0.0002 \\ -0.0002 & -2.0959 & 0.9970 & 0 & 0 \\ -0.0321 & -28.0513 & -1.9427 & 0 & 0 \\ 0 & 0 & 1 & 0 & 0 \\ 0 & 316.4283 & 0 & -316.4283 & 0 \end{bmatrix}_{5 \times 5}$$

- Disturbance (wind turbulence) matrix

$$\mathbf{B}_w = \begin{bmatrix} 0.0018 & 0.0028 & 0 & 0 \\ 0.0002 & -0.0066 & 0 & 0 \\ 0.0022 & -0.0886 & 0 & 0 \\ 0 & 0 & 0 & 0 \\ 0 & 0 & 0 & 0 \end{bmatrix}_{5 \times 4}$$

- Control matrix

$$\mathbf{B}_u = \begin{bmatrix} -5.2761 & -0.9267 & -2.1096 \\ -0.0077 & -0.1036 & -0.2498 \\ 17.6571 & -15.7595 & -34.2058 \\ 0 & 0 & 0 \\ 0 & 0 & 0 \end{bmatrix}_{5 \times 3}$$

- Output and disturbance (measurement noise) matrices

$$\mathbf{C}_z = \mathbf{C}_y = \begin{bmatrix} 0 & 1 & 0 & 0 & 0 \\ 0 & 0 & 0 & 1 & 0 \end{bmatrix}_{2 \times 5} \text{ and}$$

$$\mathbf{D}_{w1} = [0]_{2 \times 4}, \mathbf{D}_{u1} = [0]_{2 \times 3}, \mathbf{D}_{u2} = [0]_{2 \times 3}, \mathbf{D}_{w2} = [0]_{2 \times 2} \quad \mathbf{I}_{2 \times 2} \quad]_{2 \times 4}.$$

MATLAB has been used for the synthesis of the robust controller. The H_∞ controllers have been designed using the functions *loopsyn()*, *ncfsyn()* [23] and will be referenced further on as \mathbf{K}_{loop} and \mathbf{K}_{ncf} . The choice of the controller parameters was based on general rules specified in [14, 24]. For the \mathbf{K}_{ncf} the following parameters have been found:

$$\mathbf{W}_{p1} = \begin{bmatrix} \frac{s+1}{s+0.001} & 0 \\ 0 & \frac{s+1}{s+0.001} \end{bmatrix}, \mathbf{W}_{p2} = \begin{bmatrix} \frac{s+26}{s+27} & 0 \\ 0 & \frac{s+26}{s+27} \end{bmatrix}.$$

For \mathbf{K}_{loop} the cutoff frequency has been set to $\omega_c = 8$ (rad/s). The loop-shaping accuracy (3) for the selected parameters is $\gamma_{\text{loop}} = 1.435$, $\gamma_{\text{ncf}} = 2.681$. As a benchmark for the H_∞ controllers a conventional PID controller has

been designed for both controlled variables α and θ separately. E.g. the PID controller for α is given by:

$$u_\alpha = K_p \cdot e_\alpha + K_I \cdot \int e_\alpha dt + K_D \cdot \dot{e}_\alpha. \quad (4)$$

Under the assumption that for small $\Delta\alpha$: $\dot{\alpha} \approx \dot{e}_\alpha$, the controller parameters are set to $K_p = 0.0001$, $K_I = -0.1840$ and $K_D = 0.5612$.

To verify the efficiency of the suggested control algorithms, statistical analysis of the perturbed motion has been made using the Monte-Carlo method. Fig. 3 shows the experimental setup in Simulink. In this paper a statistical model of atmospheric turbulence using Dryden spectral density is realized [25]. Here two turbulence models have been implemented: a longitudinal and a lateral one. Each of these models has two input parameters: an intensity of turbulence σ_w (m/s) and a spatial wavelength L_w (m). The actuators have been modeled as static transfer elements with saturation blocks representing the lower and upper deflection limits.

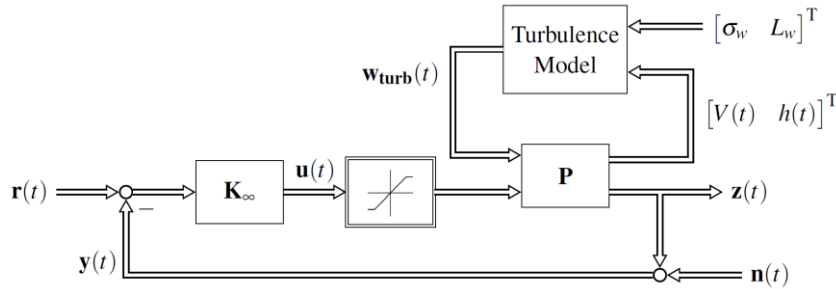


Figure 3. Structure for simulating the ADMIRE aircraft's disturbed motion in Simulink.

V. SIMULATION AND RESULTS

This section presents the simulation results obtained for the different control methods applied to the linearized ADMIRE model presented in section IV.

In Fig.4 the simulation results for a step command to α are presented. The commanded value for θ was set to 0 (relative to the equilibrium point). Here the robust controllers \mathbf{K}_{loop} and \mathbf{K}_{ncf} have been compared to the benchmark PID controller \mathbf{K}_{pid} . For further investigations the robust loop-shaping controller \mathbf{K}_{loop} has been chosen due to the better overall performance regarding the step response characteristics (see also Table I). Another advantage of the robust controller over the classical PID approach is a good decoupling of the controlled variables α and θ . As the order of the controller \mathbf{K}_{loop} with $n=15$ is quite high, in a next step a singular value based model reduction [23] has been used to reduce the order of \mathbf{K}_{loop} down to $n=7$. Fig. 5 shows the compared step responses for the reduced controller with 7th and 8th order for a perturbed plant model with aerodynamic coefficients' variation within a range of $\pm 20\%$. The robust performance for the 8th order controller (solid lines) is similar compared to the results

of the controller with full order and thus this controller has been used for the following simulations. However, if the dimensionality of the controller is reduced till 7th order, the system becomes unstable (dashed lines).

TABLE I. COMPARED QUALITY CHARACTERISTICS OF A STEP RESPONSES TO α FOR \mathbf{K}_{pid} , \mathbf{K}_{loop} AND \mathbf{K}_{ncf} .

Controller	Rise time (s)	Settling time (s)	Overshoot (%)
\mathbf{K}_{pid}	0.75	2.4	5%
\mathbf{K}_{loop}	0.47	0.6	0%
\mathbf{K}_{ncf}	0.16	2.5	0%

In a next step the robustness of the designed controller to simultaneous aerodynamic uncertainties and aerodynamic turbulence together with sensor noise has been tested. The required number of simulations for robustness analysis by the Monte-Carlo method can be estimated using rules specified in [26]. According to those rules, 150 simulations have been performed for the presented scenario. To simulate turbulence the corresponding parameters have been set to $\sigma_w = 6$ (m/s) and to $L_w = 500$ (m) [25] (Fig. 6 (a)). Measurement errors of α and θ have been considered as zero-mean white noise with a standard deviation of $\sigma_n = 0.001$ (deg).

In Fig. 6 (b) three exemplary step responses to α from the 150 performed simulations are shown. It can be seen that the responses stay within a range of $\pm 3\sigma_w$, which confirms the good robustness qualities of the reduced order controller.

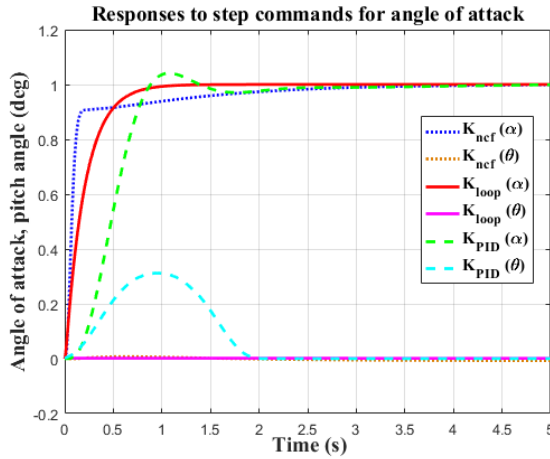


Figure 4. Comparison of step responses to α for K_{loop} , K_{ncf} and K_{pid} .

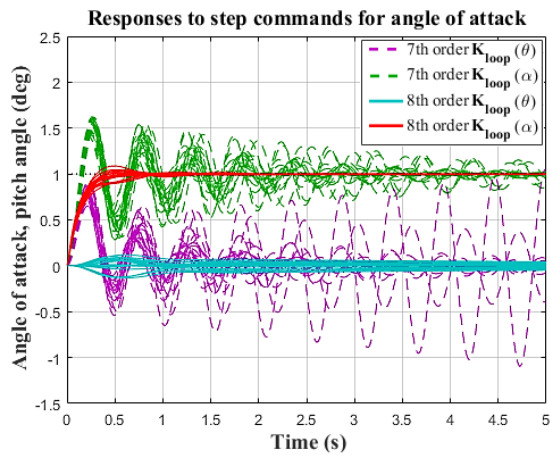


Figure 5. Response to step input command with a perturbed model of the 7th and 8th order controller

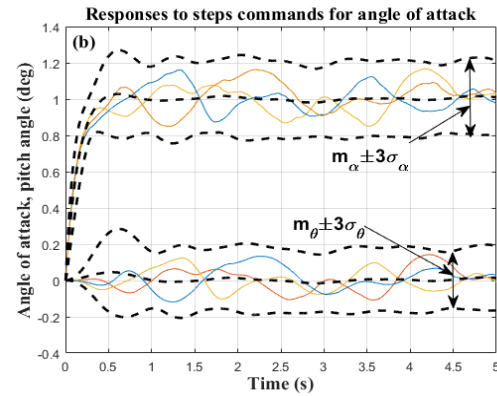
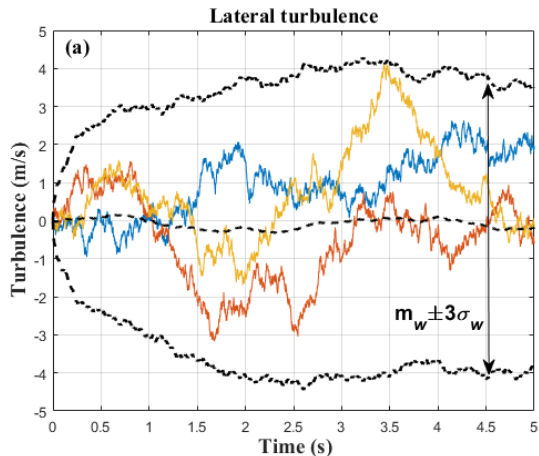


Figure 6. $\pm 3\sigma$ “tube” for lateral atmospheric turbulence gusts (a) and corresponding step responses for α with commanded $\theta=0$ (b).

For evaluation of the passive fault-tolerance capabilities of the designed control scheme degradations of each actuator with different degrees of severity in addition to the aforementioned uncertainties and disturbances have been simulated. Fig. 7 (a) shows the step responses and actuator deflections (b) for different degrees of degradation in the canards reaching from the nominal case down 80% degradation. For the sake of clarity here only the deflections of the canards and outer elevons are shown, since for the inner elevons only relatively small deviations from the fault-free case occurred. It can be seen that the AV remains stable for the different degradations although the quality of the step responses decreases drastically.

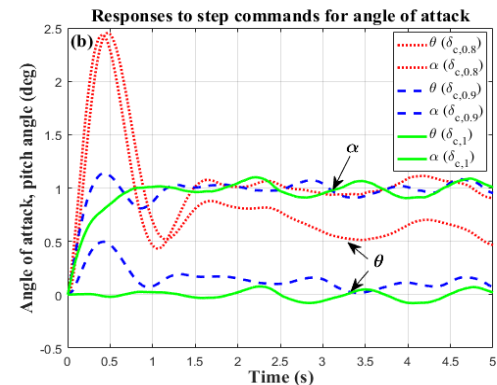
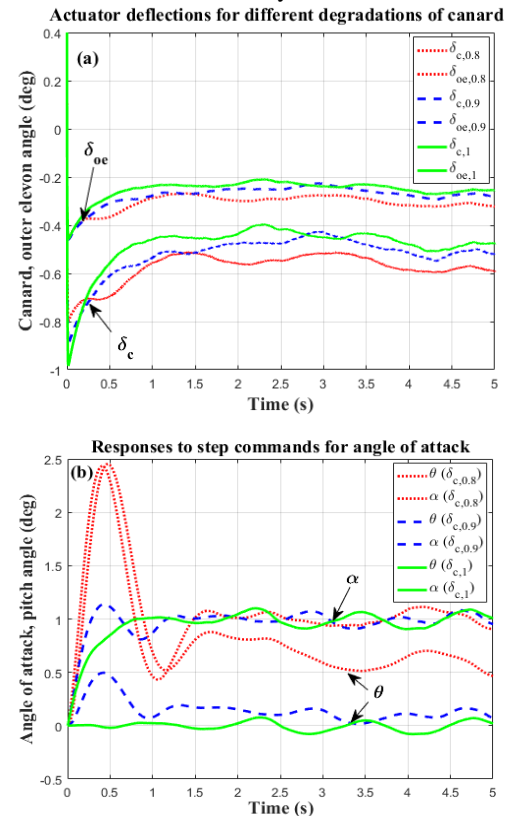


Figure 7. Actuator deflections for degradation of the canards (a) and corresponding step responses for α with commanded $\theta=0$ (b).

VI. CONCLUSION AND FUTURE WORK

In this paper, a robust control scheme for a highly agile open-loop unstable benchmark aircraft model with control input redundancy has been designed. The robust closed-loop performance in the face of parameter uncertainties and sensor noise as well as aerodynamic disturbances has been demonstrated.

Further, the analysis has been extended to the incorporation of actuator degradation faults. First results showed promising fault-tolerance capabilities within a certain range of actuator degradation with considerable worse step response characteristics. For future work a good approach would be to incorporate the good robustness properties of the designed control method into an active fault-tolerant scheme with online re-configuration in the face of severe actuator faults and failures.

ACKNOWLEDGMENT

This work was supported by Scholarship of German Academic Exchange Service (DAAD).

REFERENCES

- [1] J. A. Grauer, "Parameter uncertainty for aircraft aerodynamic modeling using recursive least squares," in *Proc. AIAA Atmospheric Flight Mechanics Conf.*, California, USA, 2016, pp. 2009.
- [2] P. Castaldi, N. Mimmo, and S. Simani, "Differential geometry based active fault tolerant control for aircraft," *Control Engineering Practice*, vol. 32, pp.227-235, 2014.
- [3] J. López, R. Dormido, S. Dormido, and J. P. Gámez, "A robust controller for an UAV flight control system," *The Scientific World Journal*, vol. 2015, 2015.
- [4] J. Ke, Z. Li, and W. Zhong, "Design of robust roll angle control system of unmanned aerial vehicles based on atmospheric turbulence attenuation," in *Proc. Intelligent Control and Automation 8th IEEE World Congress*, 2010, pp. 3746-3750.
- [5] R. Matuš, R. Prokop, and L. Pekař, "Parametric and unstructured approach to uncertainty modelling and robust stability analysis," *International Journal of Mathematical Models and Methods in Applied Sciences*, vol. 5, no. 6, pp.1011-1018, 2011.
- [6] M. Dlapa and R. Prokop, "Control of the HIMAT aircraft via algebraic μ -synthesis, in *Proc. the 7th Portuguese Conf. on Automatic Control*, 2006, pp. 11-13.
- [7] R. Kaur and J. Ohri, "H-infinity controller design for pneumatic servosystem: a comparative study," *International Journal of Automation and Control*, vol. 8, no. 3, pp.242-259, 2014.
- [8] S. Skogestad and I. Postlethwaite, "Multivariable feedback control: analysis and design," New York: Wiley, 2010.
- [9] D. C. McFarlane and K. Glover, "Robust controller design using normalised coprime factor plant descriptions," *Lecture Notes in Control and Information Sciences*, vol. 138, 1989.
- [10] D. McFarlane and K. Glover, "A loop shaping design procedure using H-infinity synthesis," *IEEE Trans. Autom. Control*, vol. 37, no. 6, pp. 759-769, 1992.
- [11] K. Zhou and J. C. Doyle, "Essentials of robust control," *Upper Saddle River, NJ: Prentice hall*, vol. 104, 1998.
- [12] K. Glover and J. C. Doyle "State-space formulae for all stabilizing controllers that satisfy an H_{∞} -norm bound and relations to relations to risk sensitivity," *Systems & Control Letters*, vol. 11, no. 3, pp. 167-172, 1988.
- [13] V. X. Le and M. G. Safonov, "Rational matrix GCD's and the design of squaring-down compensators- a state space theory," *IEEE Trans. Autom. Control*, vol. 36, no. 3, pp. 384-392, 1992.
- [14] S. Kaitwanidvilai and M. Parnichkun, "Structured robust loop shaping control for HIMAT system using swarm intelligent approach," in *Proc. the International Multi Conference of Engineers and Computer Scientists*, vol. 2, 2008.
- [15] S. I. Al Swailem, "Application of robust control in unmanned vehicle flight control system design," Ph.D. dissertation, Cranfield Univ., England, 2004.
- [16] J. P. P. Andrade and V. A. F. Campos, "Robust control of a dynamic model of an F-16 aircraft with improved damping through linear matrix inequalities," *International Journal of Computer, Electrical, Automation, Control and Information Engineering*, pp. 230-236, vol. 11, no. 2, 2017.
- [17] A. Mohamed, S. Watkins, R. Clothier, and M. Abdulrahim, "Influence of turbulence on MAV roll perturbations," *International Journal of Micro Air Vehicles*, vol. 6, no. 3, pp.175-190, 2014.
- [18] M. Blanke, M. Kinnaert, and J. Lunze, "Diagnosis and fault-tolerant control," *Springer Science & Business Media*, 2016.
- [19] F. Prochazka, H. Eduardo, and S. Klein, "Integrated fault-tolerant control of an over-actuated aircraft using optimal control allocation and robust sliding mode observers," in *Proc. 2nd IEEE Conf. on Control Technology and Applications* (in press).
- [20] L. Forsell and U. Nilsson, "Admire the aero-data model in a research environment version 4.0, model description. FOI-Totalförsvarets forskningsinstitut," 2005.
- [21] FOI. [Online]. Available: <https://www.foi.se/en/our-knowledge/aeronautics-and-air-combat-simulation/admire.html>
- [22] G. J. Balas, A. K. Packard, M. G. Safonov, and R. Y. Chiang, "Next generation of tools for robust control," in *Proc. of the 2004 American Control Conf.*, 2004, pp. 5612-5615.
- [23] R. Y. Chiang and M. G. Safonov, "MATLAB: Robust control toolbox user's guide," MathWorks, 1997.
- [24] M. Z. Babar, S. U. Ali, and M. Z. Shah, "Robust control of UAVs using H_{∞} control paradigm," in *Proc. Emerging Technologies IEEE 9th International Conf.*, 2013, pp. 1-5.
- [25] R. W. Beard and T. W. McLain, "Small unmanned aircraft: Theory and practice," Princeton university press, 2012.
- [26] E. Ventsel, "Theory of probability," Moscow: Highschool, 1999.

Maksim Trifonov received the Dipl.-Ing. degree with honors from the department of System Analysis and Control from the Moscow Aviation Institute (National Research University), Moscow, Russia in 2015. He is presently a Ph.D. student at the same university. His main research interests include optimal flight control systems and the statistical analysis of motion control systems.

Karl Frederik Prochazka received the M.Sc. degree in Electrical Engineering, Information Technology and Computer Engineering from RWTH Aachen University, Aachen, Germany in 2015. He is currently working towards the Dr.-Ing. (Ph.D.) degree at the Institute of Flight Systems and Automatic Control at Technische Universität Darmstadt, Darmstadt, Germany. His main research interests include fault-tolerant control and robust state observer design for unmanned aerial vehicles.

Saleh Krüger received the M.Sc. degree in Aerospace Mechatronics from Technische Universität Darmstadt, Darmstadt, Germany in 2017. He is currently working towards the Dr.-Ing. (Ph.D.) degree at the Institute of Flight Systems and Automatic Control at Technische Universität Darmstadt. His main research interests include increasing the operational safety and fault-tolerant control of unmanned aerial vehicles.